WRF simulations for July 2013 using NARR/GFS sources
Technical Document, last updated 17 August 2021

Matthew Garcia, Ph.D.
matt.e.garcia@gmail.com
Postdoctoral Research Associate
University of Wisconsin–Madison

in cooperation with
Joseph J. Charney, USDA Forest Service, Northern Research Station
Brian Sturtevant, USDA Forest Service, Northern Research Station
Jacques Régnière, Canadian Forest Service, Laurentian Forestry Centre
Rémi Saint-Amant, Canadian Forest Service, Laurentian Forestry Centre
and numerous others

1. Overview

We are using version 4.0.1 of the community-built Weather Research and Forecasting (WRF) model (Skamarock and Klemp, 2008; Skamarock et al., 2008; Powers et al., 2017). The Advanced Research WRF model is a widely used three-dimensional, non-hydrostatic, mesoscale atmospheric model. We applied WRF to the dynamically consistent reduction of large-scale meteorological data products from the NOAA–NCEP North American Regional Reanalysis (NARR: Mesinger et al., 2006; Luo et al., 2007) project. The NARR dataset is provided at coarse spatial and moderate temporal resolution (Δx = ~32 km and Δt = 3 h, respectively), which we reduced to meso- and micro-scales (Δx = 3 km at Δt = 60 min and Δx = 1 km at Δt = 15 min, respectively; see below) using four nested WRF grids in a telescoping configuration. Each grid has a variable vertical resolution ranging from ~57 m at the surface to ~310 m at approximately 2 km altitude, with 10 model levels within that span. Our WRF internal parameterization selections are listed below for comparison with those used previously by Sturtevant et al. (2013). We performed our WRF model simulations using the parallelized high-performance computing (HPC) cluster resources at the UW–Madison Center for High Throughput Computing (CHTC). All WRF pre- and post-processing routines were run on the distributed high-throughput computing (HTC) resources at UW–Madison CHTC.

2. WRF input (large-scale forcing) data

The NARR dataset is our primary source for historical reconstructions and analyses. For analyses within the past month and/or for forecasts, we would use the GFS dataset. The necessity, but also potential troubles, of large-scale analyses as boundary conditions for limited-area models was discussed by Warner et al. (1997).

2.1 NOAA–NCEP North American Regional Reanalysis (NARR)

Based on observations incorporated into the NCEP Eta model.

- Uses the Regional Data Assimilation System (RDAS) and includes surface precipitation observations but not land surface temperature. There are often data discontinuities at national borders. Data quality may lead to large flux residuals and dynamical imbalances in the PBL. Other issues are listed at http://www.emc.ncep.noaa.gov/mmb/rreanl/faq.html
- Analysis product is 3-hourly with ~32-km horizontal grid spacing and 30 vertical layers.
- Analyses available from 1 January 1979. The newest products are usually posted in month-long chunks with a 1- to 2-week delay.
- Data product is in at least 3 parts: "3D," "sfc," and "flx." These get combined during the WRF Preprocessing System (WPS) procedure, described below. The data files are located at NCAR/UCAR and requires an account to download. NOTE: there is a "combined" NARR data product available at the same site and from NOAA/NCEI (https://www.ncdc.noaa.gov/data-access/model-data/model-datasets/north-american-regional-reanalysis-narr) but it doesn't work properly with the WPS.

2.1.1 Links

https://rda.ucar.edu/datasets/ds608.0/ (primary download site)
https://www.esrl.noaa.gov/psd/data/gridded/data.narr.html
http://www.emc.ncep.noaa.gov/mmb/rreanl/

2.1.2 References (with bulleted annotations)

Mesinger, F., G. DiMego, E. Kalnay, K. Mitchell, P.C. Shafran, W. Ebisuzaki, D. Jović, J. Woollen, E. Rogers, E.H. Berbery, M.B. Ek, Y. Fan, R. Grumbine, W. Higgins, H. Li, Y. Lin, G. Manikin, D. Parrish, and W. Shi, 2006: North American Regional Reanalysis. *Bull. Amer. Meteor. Soc.*, **87**, 343-360, http://doi.org/10.1175/BAMS-87-3-343.

- Standard reference for NARR origin

Luo, Y., E.H. Berbery, K.E. Mitchell, and A.K. Betts, 2007: Relationships between land surface and near-surface atmospheric variables in the NCEP North American Regional Reanalysis. *J. Hydrometeor.*, **8**, 1184-1203, http://doi.org/10.1175/2007JHM844.1.

- Excellent brief description of the essentials of the NARR modeling procedure and several assimilated data sources

2.2 NCEP Global Forecast System (GFS)

Global spectral model in operational use for analysis and forecasting

- Uses the Noah land surface model (LSM).
- Used as the atmospheric model in the NCEP Climate Forecast System (CFS).
- Uses the Global Data Assimilation System (GDAS) with satellite, conventional (airborne, surface, balloon soundings), and radar data source inputs via the Gridpoint Statistical Interpolation (GSI) 3D variational data assimilation (3DVAR) methodology.
- Analysis product is 6-hourly with 0.5-degree horizontal grid spacing (~33 km at ~48ºN) and 27 vertical layers. Forecast products out to 8 days are available on the same grid at 3-hour intervals.
- Analyses available from 1 January 2007. The newest products are usually posted the same day as their generation.

2.2.1 Links

http://www.emc.ncep.noaa.gov/GFS/
https://www.ncdc.noaa.gov/data-access/model-data/model-datasets/global-forcast-system-gfs
http://www.emc.ncep.noaa.gov/index.php?branch=GFS

2.2.2 References

Saha, S., S. Nadiga, C. Thiaw, J. Wang, W. Wang, Q. Zhang, H.M. Van den Dool, H. Pan, S. Moorthi, D. Behringer, D. Stokes, M. Peña, S. Lord, G. White, W. Ebisuzaki, P. Peng, and P. Xie, 2006: The NCEP Climate Forecast System. *J. Climate*, **19**, 3483-3517, http://doi.org/10.1175/JCLI3812.1.

Yang, F., H. Pan, S.K. Krueger, S. Moorthi, and S.J. Lord, 2006: Evaluation of the NCEP Global Forecast System at the ARM SGP site. *Mon. Wea. Rev.*, **134**, 3668-3690, http://doi.org/10.1175/MWR3264.1.

Kleist, D.T., D.F. Parrish, J.C. Derber, R. Treadon, W. Wu, and S. Lord, 2009: Introduction of the GSI into the NCEP Global Data Assimilation System. *Wea. Forecast.*, **24**, 1691-1705, http://doi.org/10.1175/2009WAF2222201.1.

Werth, D., and A. Garrett, 2011: Patterns of land surface errors and biases in the Global Forecast System. *Mon. Wea. Rev.*, **139**, 1569-1582, http://doi.org/10.1175/2010MWR3423.1.

3. Weather Research and Forecasting (WRF-ARW) model v4.0.1

WRF is now available via GitHub at https://github.com/wrf-model. This document previously described the use of WRF-ARW v3.9.1.1. Version 4 of the WRF modeling system was released via GitHub on 8 June 2018 and some bug fixes contributed by the user community led to the release of Version 4.0.1 via GitHub on 2 October 2018.

The complete WRFv4 User's Guide is available online at
http://www2.mmm.ucar.edu/wrf/users/docs/user_guide_v4/v4.0/contents.html
and as a pdf (454 pages) at
http://www2.mmm.ucar.edu/wrf/users/docs/user_guide_V4/WRFUsersGuide.pdf.

3.1 WRF Preprocessing System (WPS) configuration

- Many static geographic fields (topography, land cover, etc.) are updated from WRF v3.
- MODIS/IGBP-based land cover classes (listed in the Annotated Bibliography) with inland lakes as a separate land cover category.
    - Typically, inland lake temperatures are generated by interpolating/extrapolating SST, often leading to too-warm or too-cold biases. Instead, we are using a WPS function that calculates daily mean surface temperatures at inland lake locations (from the NARR/GFS input dataset) for use as lake surface temperatures.
- MODIS-based average monthly albedo, LAI, and FPAR/greenness fraction (see references for background information).

- Setup does *not* include SBW defoliation effects on LAI/greenness maps; this is a topic for further discussion and testing.
- Executing the WPS procedure on a single processor at CHTC is now fully scripted and submitted as a standard computing job, taking a few hours for a 1.5-day simulation.

3.2 Weather Research and Forecasting (WRF-ARW) model configuration

- Compiled for distributed memory parallel (dmpar) system using MPICH
- 4 nested grids @ 27-, 9-, 3-, and 1-km grid spacing in telescoping configuration (see map and table below) with 1-way nesting.
- Grid 4 fully covers the Val d'Irène (XAM) radar observation area (red box in map).
- Model period covers 00 UTC on day 1 through 12 UTC on day 2.
    - 12 hours spin-up on day 1, then 24 hours in the overnight migration window, with the last 12 hours (on day 2) overlapping with the spin-up period for the next day.
- 40 vertical levels with 11 levels (10 layers) in the lowest 2 km, ranging in thickness from 56 to 320 m.
- Noah-MP land surface model with 4 soil layers and dynamic vegetation, using albedo, LAI and greenness fraction (via FPAR) provided by MODIS-based monthly averages.
- 21 total land cover categories (20 MODIS/IGBP/Noah-MP classes + inland lakes, as for WPS).
- Cloud and precipitation microphysics via Thompson scheme.
- RRTMG longwave and shortwave radiation schemes, updated every 10 minutes.
- Grid cell cloud fraction by Xu–Randall method.
- Surface layer by revised MM5 surface layer scheme.
- Boundary layer physics by YSU non-local scheme, with topographic correction for surface winds to represent drag from sub-grid topography and enhanced flow at hilltops, and top-down BL mixing is driven by radiative cooling, all updated at every time step.
- Cumulus parameterization by Grell–Freitas scheme on Grids 1-3, updated on every time step. *No cumulus parameterization is applied to Grid 4 at 1 km grid spacing*.
- Additional parameter specifications for diffusion, damping at upper boundary, etc.

Table 1: WRF configuration details (see below for annotated bibliography and references)

Dynamical (physics) core:	Advanced Research WRF v4.0.1
Longwave radiation transfer:	RRTMG
Shortwave radiation transfer:	RRTMG
Convective parameterization:	Grell–Freitas (except on 1-km grid)
Cloud/precipitation microphysics:	Thompson
Boundary layer:	YSU non-local scheme
Surface layer:	MM5 formulation
Horizontal diffusion:	Simple, with K via 2-D deformation
Land surface model:	Noah-MP
Topography:	USGS GMTED2010
Land cover:	Modified MODIS/IGBP categories
Vegetation (greenness, LAI, albedo):	NASA MODIS
Large-scale meteorological reanalysis:	North American Regional Reanalysis

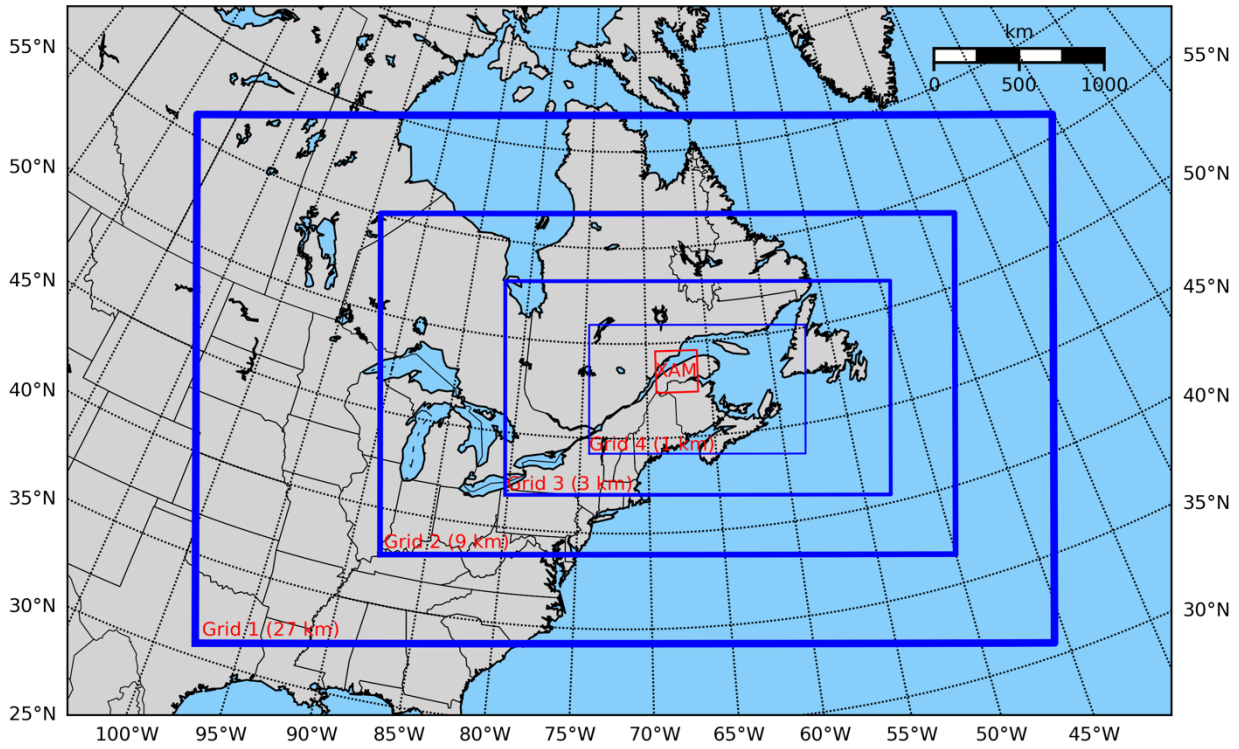

Figure 1: Geography of WRF nested/telescoping grids.

Table 2: Simulation grid parameters

	Grid 1	**Grid 2**	**Grid 3**	**Grid 4**
Δx [km]	27	9	3	1
Δt [s]	108	36	12	4
Model Points (x, y)	182 x 113	364 x 217	730 x 406	1228 x 733
Distance (x, y) [km]	4914 x 3051	3276 x 1953	2190 x 1218	1228 x 733
Model Levels (z)	40	40	40	40
Cloud parameterization	Grell–Freitas	Grell–Freitas	Grell–Freitas	none
Simulation period	36 h	36 h	36 h	36 h
Output interval	6 h	3 h	1 h	15 m
Retained output files per sim	4	7	19	73
Output raw file size	79 MB	304 MB	1.14 GB	3.48 GB
Output reduced file size	-	-	141 MB	428 MB
Total output per sim ~312 GB	319 MB	2.08 GB	24.4 GB	285.4 GB

Table 3: WRF 40-level configuration: layer base heights and thicknesses

Level	Level Height [m]	Layer Thickness [m]
1	0.0	—
2	56.6	56.6
3	137.9	81.4
4	244.7	106.8
5	377.6	132.9
6	546.3	168.7
7	761.1	214.8
8	1016.2	255.0
9	1316.2	300.0
10	1625.5	309.3
11	1944.7	319.2

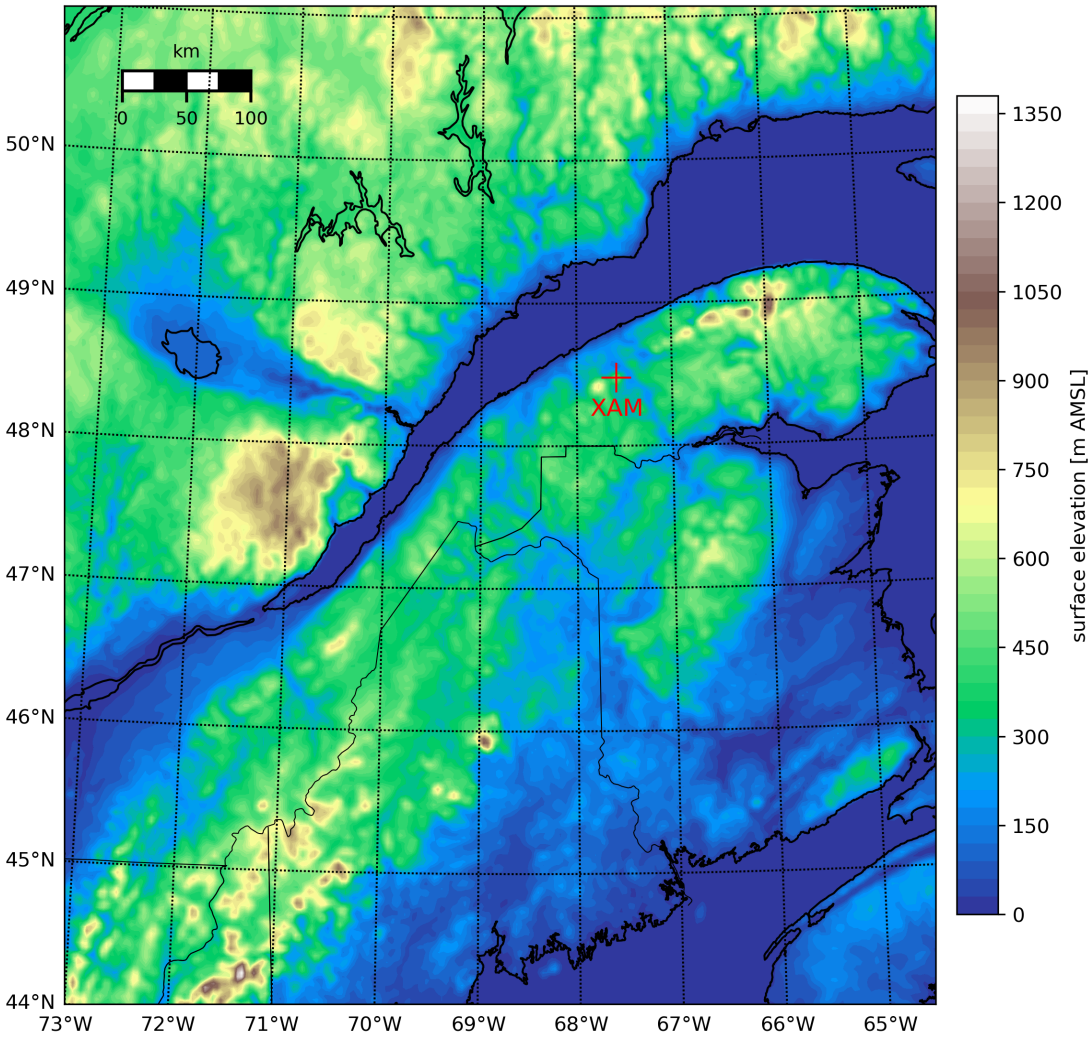

Figure 2: topography on Grid 3.

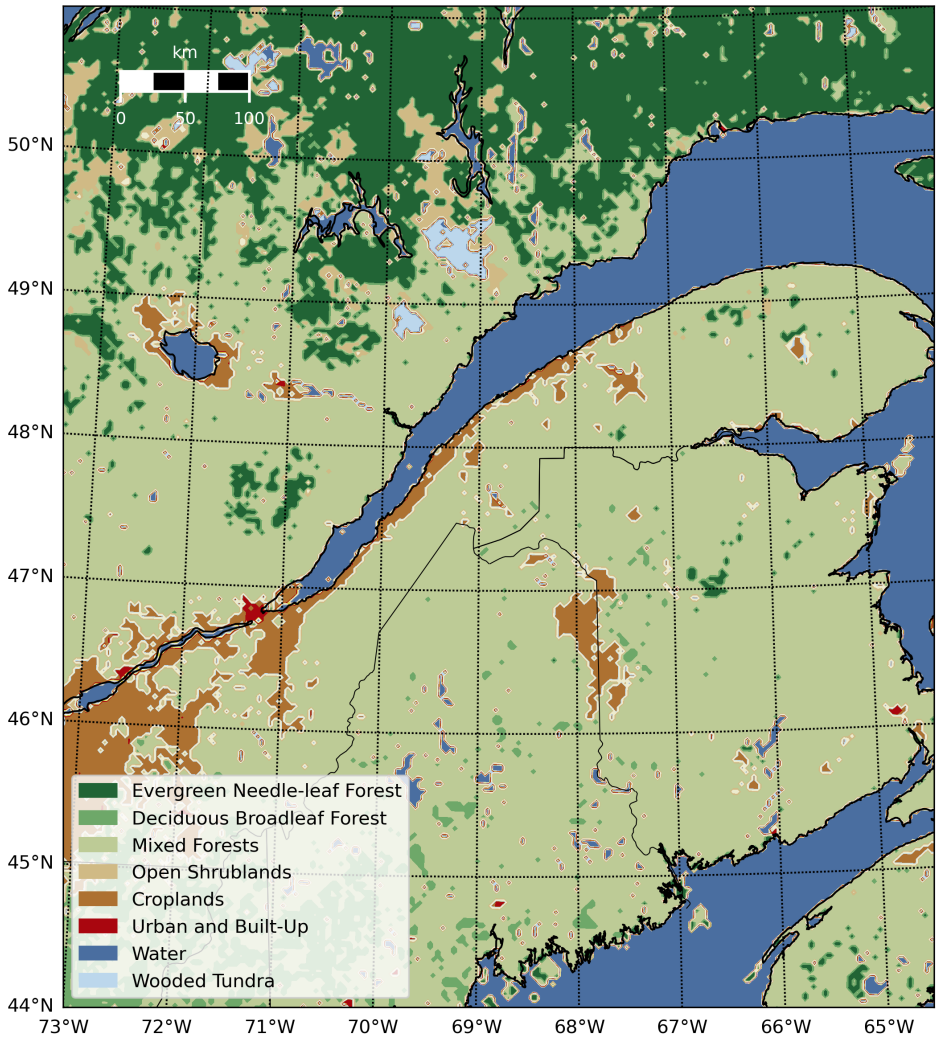

Figure 3: Modified MODIS/IGBP land cover categories on Grid 3. Colors match equivalent categories in the U.S. National Land Cover Database (NLCD; https://www.mrlc.gov/).

Table 4: Modified MODIS/IGBP land cover categories

Category	Description	Category	Description
1	Evergreen Needle-leaf Forest	11	Permanent Wetlands
2	Evergreen Broadleaf Forest	12	Croplands
3	Deciduous Needle-leaf Forest	13	Urban and Built-Up
4	Deciduous Broadleaf Forest	14	Cropland/Natural Veg. Mosaic
5	Mixed Forests	15	Snow and Ice
6	Closed Shrublands	16	Barren or Sparsely Vegetated
7	Open Shrublands	17	Water
8	Woody Savannas	18	Wooded Tundra
9	Savannas	19	Mixed Tundra
10	Grasslands	20	Barren Tundra
		21	*Inland Lakes (separate from Water)*

3.3 WRF model operation

My workflow at UW–Madison CHTC has several steps using the WRF-MPI package compiled the same way on both HTC and HPC computing systems, and then a post-processing step to reduce the output dataset for portability:

1. WRF Preprocessing System (WPS) execution to build WRF model input files, primarily a single-CPU process, is fully scripted on the HTC side.
2. WRF set-up to build the initial conditions for each simulation grid and the boundary conditions for the outer grid over the entire simulation time period, primarily a single-CPU process with large memory requirements (>80 GB RAM), is fully scripted on the HTC side.
3. WRF-MPI simulation execution is a multi-CPU synchronous parallel process, fully scripted on the HPC side. Currently these simulations use 150 CPUs each (15 nodes, 10 CPUs per node) with ~6 GB RAM per CPU.
4. Output intervals are as designated in the table above. Only grid-3 and -4 outputs for the latter 27 hours of each simulation are retained (09 UTC on day 1 through 12 UTC on day 2).
5. WRF output is transferred to the HTC side where I run post-processing and data reduction procedure for Earth-relative wind corrections and to remove other variables and levels not needed for ATM execution. The variables retained for use in pyATM are listed below.

3.4 Post-processing Procedures

Following completion of the WRF simulation, each output NetCDF file on Grids 3 and 4 is post-processed to reduce the contained variables and upper air levels to those that will be used in the SBW-ATM procedure. Post-processing uses ***wrf-python*** (https://github.com/NCAR/wrf-python) and the ***wrfcube*** library (http://github.com/mheikenfeld/wrfcube). Wind rotation to Earth-relative components uses an online example (https://atmos.washington.edu/~ovens/wrfwinds.html).

The following WRF output variables are retained for use in SBW–pyATM simulations:

- Topography, land use category index, and vegetation LAI
- Geopotential height [m] of model layers at all grid points
- Air temperature [°C] at surface (T_{2m}) and upper-air levels
- Relative humidity [%] at surface (to be implemented)
- Atmospheric pressure [hPa] at surface (P_{sfc}) and upper-air levels
- Precipitation [mm/h] at surface and cloud liquid water [g/kg] at upper-air levels
- U (Earth-relative eastward wind component) [m/s] at surface (U_{10m}) and upper-air levels
- V (Earth-relative northward wind component) [m/s] at surface (V_{10m}) and upper-air levels
- W (vertical wind component) [m/s] at upper-air levels (no surface field)

Wind variables are resampled to an unstaggered grid for conformity, and upper-air variables are subset to the lowest 11 model levels (~2.0 km; see table below) since we don't expect SBW-ATM flights above that height. The data reduction procedure can also subset the WRF output spatially to areas smaller than WRF Grid 3 or 4, if desired.

4. Additional Notes and Considerations

- Review with Jay Charney led to a change in the way WRF treats the telescoping grids from 2-way nesting to 1-way nesting, so that information on the coarser grids would remain valid (esp. grid 3 with the Labrador and Newfoundland areas of interest).
- The outer grid covers an area as large as possible while still fitting within the NARR coverage limits over the North Atlantic Ocean, and generally large enough to reduce any effect of adjustment to boundary conditions imposed by NARR/GFS input.
- Grid 3 covers southern Québec and Newfoundland, including the 2013 Québec defoliation areas shown in the maps provided by Rémi Saint-Amant.
- Grid 4 covers the center of defoliation activity along the Côte Nord and the Val d'Irène (XAM) radar area at approximately the same spatial resolution as the provided radar dataset from Yan Boulanger.
- Instead of a long simulation period covering the dates of interest, at least one reference in the literature (Lo et al., 2008; Lucas-Picher et al., 2013) and Jay's advice recommended shorter simulation periods with more frequent re-initialization from NARR/GFS conditions for a more faithful and accurate representation of those analyses. Repeated 1.5-day simulations, with a slight overlap to provide some spin-up time for individual simulation periods, can cover all of the main dates of SBW migration indicated in Frédéric's summary of the 2013 radar data.
- The spin-up period, 9 hours at the beginning of each simulation, was selected to provide for a leading night before we would consider the data "valid" for simulation of SBW moth flight events. While we could have gone without a spin-up period, this provided time for nocturnal boundary layer (NBL) establishment (after sunset the previous night) and erosion (around sunrise) that would be important in establishing the circadian cycle at the smallest scales, where we are interested in those details.
- Review with Rémi and Jay led to revisions in the post-processing procedure, including rotation of the horizontal wind vectors from WRF-grid-relative (on the WRF Lambert conformal conic grid) to Earth-relative (geographic/unprojected) for proper use with the SBW–pyATM model. Care must be taken to ensure that any map or display must then convert the Earth-relative winds into the map's projection system.
- I've been re-reading Stull's text (*An Introduction to Boundary Layer Meteorology*, referenced below, from my graduate school days), especially reviewing nocturnal BL (NBL) dynamics. In the stable NBL, turbulence is restricted such that it takes several hours for information regarding some disturbance (perturbation, e.g. a heat plume) at the surface to reach the top of the NBL. In addition, the NBL doesn't occupy the full depth of the daytime BL, but only the lowest few hundred meters, with a "residual layer" (left over from the daytime BL) above. Conversely, the daytime BL (and thus the nighttime residual layer) is well-mixed and the turbulence is not so restricted, so that the information from some disturbance/perturbation at the surface can reach the top of the BL within ~15 minutes. This was part of the reasoning that led to my selection of the Grid 4 output interval listed above.
- The other part of that reasoning was that I'd been thinking about the timing of WRF output provision to the ATM model, and whether hourly output is frequent enough.

Around sunset, BL dynamics can evolve and change rapidly, on a time span that is more like the temporal frequency of the radar data (10 minutes) against which we are calibrating ATM parameters. I don't think this means that we need to provide WRF output to ATM on a 10-minute cycle, but it's likely a 15-minute cycle could improve how the timing and accuracy of changes in the BL are communicated to the ATM model and its own results. Rémi says that BioSIM-ATM currently assumes/accepts sub-hourly meteorological inputs in its simulation process. This might be a rich area to explore with sensitivity testing, *e.g.*, ATM results accuracy using 5-, 10-, 15-, 30- and 60-minute input intervals.

- For some background and comparison, I have been looking at the combination of WRF with CMAQ, the Community Multiscale Air Quality model in common use at the USEPA. Like our intended combination of WRF with ATM, CMAQ takes meteorological outputs and runs separately. The "standard" frequency of WRF output to CMAQ input is hourly (see https://github.com/USEPA/CMAQ/blob/5.2/DOCS/User_Manual/CMAQ_OGD_ch04_science.md#mcip-meteorology-chemistry-interface-processor). I've yet to find any studies on whether more accurate results from CMAQ are obtained with more frequent meteorological inputs, but I have emailed Jonathan Pleim (USEPA) regarding whether he or anyone he knows has worked on that question.
- The WRF–CMAQ connection is also useful for a couple of references (Ran et al., 2015 and 2016, listed below) regarding the use of MODIS products (albedo, vegetation LAI and FPAR/greenness) that are indicated above as WPS/WRF model inputs, replacing standard Noah/Noah-MP look-up-tables based on (coarse) land cover categories for those parameter values.
- For higher-resolution simulations, I'm learning more about the large eddy simulation (LES) capabilities in WRF but have not implemented any of those methods yet.

5. Annotated Bibliography

NOTE: block quotes are from the WRF v4 Model User's Guide at http://www2.mmm.ucar.edu/wrf/users/docs/user_guide_v4/v4.0/users_guide_chap5.html

5.1 Background on WRF-ARW

Skamarock, W.C., J.B. Klemp, J. Dudhia, D.O. Gill, D.M. Barker, M.G. Duda, X.-Y. Huang, W. Wang, and J.G. Powers, 2008: *A description of the Advanced Research WRF version 3*. NCAR Tech. Note NCAR/TN-475+STR, 113 pp., http://doi.org/10.5065/D68S4MVH.

- The official WRF v3 technical document

Skamarock, W.C., and J.B. Klemp, 2008: A time-split nonhydrostatic atmospheric model for weather research and forecasting applications. *J. Comput. Phys.*, **227**, 3465-3485, http://doi.org/10.1016/j.jcp.2007.01.037.

- Fundamental reference describing the ARW dynamical core

LeMone, M.A., F. Chen, M. Tewari, J. Dudhia, B. Geerts, Q. Miao, R.L. Coulter, and R.L. Grossman, 2010a: Simulating the IHOP_2002 fair-weather CBL with the WRF-ARW–

Noah modeling system. Part I: Surface fluxes and CBL structure and evolution along the eastern track. *Mon. Wea. Rev.*, **138**, 722-744, http://doi.org/10.1175/2009MWR3003.1.

- See also *LeMone et al. [2008]* in the Noah LSM section above

LeMone, M.A., F. Chen, M. Tewari, J. Dudhia, B. Geerts, Q. Miao, R.L. Coulter, and R.L. Grossman, 2010b: Simulating the IHOP_2002 fair-weather CBL with the WRF-ARW–Noah modeling system. Part II: Structures from a few kilometers to 100 km across. *Mon. Wea. Rev.*, **138**, 745-764, http://doi.org/10.1175/2009MWR3004.1.

Trier, S.B., M.A. LeMone, F. Chen, and K.W. Manning, 2011: Effects of surface heat and moisture exchange on ARW-WRF warm-season precipitation forecasts over the central United States. *Wea. Forecast.*, **26**, 3-25, http://doi.org/10.1175/2010WAF2222426.1.

Powers, J.G., J.B. Klemp, W.C. Skamarock, C.A. Davis, J. Dudhia, D.O. Gill, J.L. Coen, D.J. Gochis, R. Ahmadov, S.E. Peckham, G.A. Grell, J. Michalakes, S. Trahan, S.G. Benjamin, C.R. Alexander, G.J. Dimego, W. Wang, C.S. Schwartz, G.S. Romine, Z. Liu, C. Snyder, F. Chen, M.J. Barlage, W. Yu, and M.G. Duda, 2017: The Weather Research and Forecasting model: Overview, system efforts, and future directions. *Bulletin of the American Meteorological Society*, **98**, 1717–1737, http://doi.org/10.1175/BAMS-D-15-00308.1.

5.2 Cumulus scheme

"Grell-Devenyi (GD) ensemble scheme: Multi-closure, multi-parameter, ensemble method with typically 144 sub-grid members (moved to option 93 in V3.5)."

"Grell-Freitas (GF) scheme (3): An improved GD scheme that tries to smooth the transition to cloud-resolving scales, as proposed by Arakawa et al. (2004). New in Version 3.5."

Grell, G.A., Y. Kuo, and R.J. Pasch, 1991: Semiprognostic tests of cumulus parameterization schemes in the middle latitudes. *Mon. Wea. Rev.*, **119**, 5-31, http://doi.org/10.1175/1520-0493(1991)119<0005:STOCPS>2.0.CO;2.

Grell, G.A., 1993: Prognostic evaluation of assumptions used by cumulus parameterizations. *Mon. Wea. Rev.*, **121**, 764-787, http://doi.org/10.1175/1520-0493(1993)121<0764:PEOAUB>2.0.CO;2.

Grell, G.A., and D. Dévényi, 2002: A generalized approach to parameterizing convection combining ensemble and data assimilation techniques. *Geophys. Res. Lett.*, **29**, 1693, http://doi.org/10.1029/2002GL015311.

Arakawa, A., 2004: The cumulus parameterization problem: Past, present, and future. *J. Climate*, **17**, 2493-2525, http://doi.org/10.1175/1520-0442(2004)017<2493:RATCPP>2.0.CO;2.

Grell, G.A., and S.R. Freitas, 2014: A scale and aerosol aware stochastic convective parameterization for weather and air quality modeling. *Atmos. Chem. Phys.*, **14**, 5233-5250, http://doi.org/10.5194/acp-14-5233-2014.

Fowler, L.D., W.C. Skamarock, G.A. Grell, S.R. Freitas, and M.G. Duda, 2016: Analyzing the Grell–Freitas convection scheme from hydrostatic to nonhydrostatic scales within a global model. *Mon. Wea. Rev.*, **144**, 2285-2306, http://doi.org/10.1175/MWR-D-15-0311.1.

5.3 Microphysics scheme

> "New Thompson et al. scheme: A new scheme with ice, snow and graupel processes suitable for high-resolution simulations (8). This adds rain number concentration and updates the scheme from the one in Version 3.0. New in Version 3.1."

Thompson, G., P.R. Field, R.M. Rasmussen, and W.D. Hall, 2008: Explicit forecasts of winter precipitation using an improved bulk microphysics scheme. Part II: Implementation of a new snow parameterization. *Mon. Wea. Rev.*, **136**, 5095-5115, http://doi.org/10.1175/2008MWR2387.1.

5.4 Radiation schemes

> "RRTM scheme (*ra_lw_physics* = 1): Rapid Radiative Transfer Model. An accurate scheme using look-up tables for efficiency. Accounts for multiple bands, and microphysics species. For trace gases, the volume-mixing ratio values for CO_2=330e-6, N_2O=0. and CH_4=0. in pre-V3.5 code; in V3.5, CO_2=379e-6, N_2O=319e-9 and CH_4=1774e-9. See section 2.3 for time-varying option."

> "RRTMG scheme (4): A new version of RRTM added in Version 3.1. It includes the MCICA method of random cloud overlap. For major trace gases, CO_2=379e-6, N_2O=319e-9, CH_4=1774e-9. See section 2.3 for the time-varying option. In V3.7, a fast version is introduced as option 24."

> "RRTMG shortwave. A new shortwave scheme with the MCICA method of random cloud overlap (4). New in Version 3.1. In V3.7, a fast version is introduced as option 24."

Iacono, M.J., J.S. Delamere, E.J. Mlawer, M.W. Shephard, S.A. Clough, and W.D. Collins, 2008: Radiative forcing by long-lived greenhouse gases: Calculations with the AER radiative transfer models. *J. Geophys. Res.*, **113**, D13103, http://doi.org/10.1029/2008JD009944.

5.5 Surface layer scheme

> "Revised MM5 surface layer scheme (option 11 prior to V3.6, renamed to option 1 since V3.6): Remove limits and use updated stability functions. New in Version 3.4. (Jimenez et al. MWR 2012). In V3.7, the code is sped up to give similar timing as with the old MM5 scheme. The thermal and moisture roughness lengths (or exchange coefficients for heat and moisture) over ocean are changed to COARE 3 formula (Fairall et al. 2003) in V3.7."

Fairall, C.W., E.F. Bradley, J.E. Hare, A.A. Grachev, and J.B. Edson, 2003: Bulk parameterization of air–sea fluxes: Updates and verification for the COARE algorithm. *J.*

Climate, **16**, 571-591, http://doi.org/10.1175/1520-0442(2003)016<0571:BPOASF>2.0.CO;2.

Horvath, K., D. Koracin, R. Vellore, J.H. Jiang, and R. Belu, 2012: Sub-kilometer dynamical downscaling of near-surface winds in complex terrain using WRF and MM5 mesoscale models. *J. Geophys. Res. Atmos.*, **117**, http://doi.org/10.1029/2012jd017432.

Jiménez, P.A., J. Dudhia, J.F. González-Rouco, J. Navarro, J.P. Montávez, and E. García-Bustamante, 2012: A revised scheme for the WRF surface layer formulation. *Mon. Wea. Rev.*, **140**, 898-918, http://doi.org/10.1175/MWR-D-11-00056.1.

- Note this formulation fits well with the YSU boundary layer scheme, especially improvements to account for topography and BL stability by Jiménez, Dudhia, others.

5.6 Boundary layer scheme

"Yonsei University scheme: Non-local-K scheme with explicit entrainment layer and parabolic K profile in unstable mixed layer (bl_pbl_physics = 1).

- topo_wind: = 1: Topographic correction for surface winds to represent extra drag from sub-grid topography and enhanced flow at hill tops (Jimenez and Dudhia, JAMC 2012). Works with YSU PBL only. New in Version 3.4.
- ysu_topdown_pblmix: = 1: option for top-down mixing driven by radiative cooling. New in V3.7."

Stull, R., 1988: *An Introduction to Boundary Layer Meteorology*. Kluwer Academic Publishers, 670 pp., ISBN 978-90-277-2769-4.

- Fundamental reference for any BL study.

Hong, S., Y. Noh, and J. Dudhia, 2006: A new vertical diffusion package with an explicit treatment of entrainment processes. *Mon. Wea. Rev.*, **134**, 2318-2341, http://doi.org/10.1175/MWR3199.1.

Hu, X., J.W. Nielsen-Gammon, and F. Zhang, 2010: Evaluation of three planetary boundary layer schemes in the WRF model. *J. Appl. Meteor. Climatol.*, **49**, 1831-1844, http://doi.org/10.1175/2010JAMC2432.1.

Jiménez, P.A., J.F. González-Rouco, E. García-Bustamante, J. Navarro, J.P. Montávez, J.V. de Arellano, J. Dudhia, and A. Muñoz-Roldan, 2010: Surface wind regionalization over complex terrain: Evaluation and analysis of a high-resolution WRF simulation. *J. Appl. Meteor. Climatol.*, **49**, 268-287, http://doi.org/10.1175/2009JAMC2175.1.

Jiménez, P.A. and J. Dudhia, 2012: Improving the representation of resolved and unresolved topographic effects on surface wind in the WRF model. *J. Appl. Meteor. Climatol.*, **51**, 300-316, http://doi.org/10.1175/JAMC-D-11-084.1.

Jiménez, P.A., J. Dudhia, J.F. González-Rouco, J. Navarro, J.P. Montávez, and E. García-Bustamante, 2012: A revised scheme for the WRF surface layer formulation. *Mon. Wea. Rev.*, **140**, 898-918, http://doi.org/10.1175/MWR-D-11-00056.1.

Shin, H.H., S. Hong, and J. Dudhia, 2012: Impacts of the lowest model level height on the performance of planetary boundary layer parameterizations. *Mon. Wea. Rev.*, **140**, 664-682, http://doi.org/10.1175/MWR-D-11-00027.1.

Hu, X.-M., P.M. Klein, and M. Xue, 2013: Evaluation of the updated YSU planetary boundary layer scheme within WRF for wind resource and air quality assessments. *J. Geophys. Res. Atmos.*, **118**, http://doi.org/10.1002/jgrd.50823.

Jiménez, P.A. and J. Dudhia, 2013: On the ability of the WRF model to reproduce the surface wind direction over complex terrain. *J. Appl. Meteor. Climatol.*, **52**, 1610-1617, http://doi.org/10.1175/JAMC-D-12-0266.1.

Jiménez, P.A., J. Dudhia, J.F. González-Rouco, J.P. Montávez, E. García-Bustamante, J. Navarro, J. Vilà-Guerau de Arellano, and A. Muñoz-Roldán, 2013: An evaluation of WRF's ability to reproduce the surface wind over complex terrain based on typical circulation patterns. *J. Geophys. Res. Atmos.*, **118**, 7651-7669, http://doi.org/10.1002/jgrd.50585.

Lorente-Plazas, R., P.A. Jiménez, J. Dudhia, and J.P. Montávez, 2016: Evaluating and improving the impact of the atmospheric stability and orography on surface winds in the WRF model. *Mon. Wea. Rev.*, **144**, 2685-2693, http://doi.org/10.1175/MWR-D-15-0449.1.

5.7 Noah-MP land surface model

"Noah Land Surface Model: Unified NCEP/NCAR/AFWA scheme with soil temperature and moisture in four layers, fractional snow cover and frozen soil physics. New modifications are added in Version 3.1 to better represent processes over ice sheets and snow-covered area."

"Noah-MP (multi-physics) Land Surface Model: uses multiple options for key land-atmosphere interaction processes. Noah-MP contains a separate vegetation canopy defined by a canopy top and bottom with leaf physical and radiometric properties used in a two-stream canopy radiation transfer scheme that includes shading effects. Noah-MP contains a multi-layer snow pack with liquid water storage and melt/refreeze capability and a snow-interception model describing loading/unloading, melt/refreeze, and sublimation of the canopy-intercepted snow. Multiple options are available for surface water infiltration and runoff, and groundwater transfer and storage including water table depth to an unconfined aquifer. Horizontal and vertical vegetation density can be prescribed or predicted using prognostic photosynthesis and dynamic vegetation models that allocate carbon to vegetation (leaf, stem, wood and root) and soil carbon pools (fast and slow). New in Version 3.4. (Niu et al. 2011)"

"usemonalb: uses monthly albedo fields from geogrid, instead of table values."

"rdlai2d: uses monthly LAI data from geogrid (new in V3.6)."

Chen, F., H. Kusaka, R. Bornstein, J. Ching, C.S.B. Grimmond, S. Grossman-Clarke, T. Loridan, K.W. Manning, A. Martilli, S. Miao, D. Sailor, F.P. Salamanca, H. Taha, M. Tewari, X. Wang, A.A. Wyszogrodzki, and C. Zhang, 2011: The integrated WRF/urban modelling system: Development, evaluation, and applications to urban environmental problems. *Int. J. Climatol.*, **31**, 273-288, http://doi.org/10.1002/joc.2158.

Niu, G.-Y., Z.-L. Yang, K.E. Mitchell, F. Chen, M.B. Ek, M. Barlage, A. Kumar, K. Manning, D. Niyogi, E. Rosero, M. Tewari, and Y. Xia, 2011: The community Noah land surface model with multiparameterization options (Noah-MP): 1. Model description and

evaluation with local-scale measurements, *J. Geophys. Res.*, **116**, D12109, http://doi.org/10.1029/2010JD015139.

Yang, Z.-L., G.-Y. Niu, K.E. Mitchell, F. Chen, M.B. Ek, M. Barlage, L. Longuevergne, K. Manning, D. Niyogi, M. Tewari, and Y. Xia, 2011: The community Noah land surface model with multiparameterization options (Noah-MP): 2. Evaluation over global river basins. *J. Geophys. Res.*, **116**, D12110, http://doi.org/10.1029/2010JD015140.

Salamanca, F., Y. Zhang, M. Barlage, F. Chen, A. Mahalov, and S. Miao, 2018: Evaluation of the WRF-urban modeling system coupled to Noah and Noah-MP land surface models over a semiarid urban environment. *J. Geophys. Res. Atmos.*, **123**, http://doi.org/10.1002/2018JD028377.

5.8 Background on Noah LSM

Pan, H.-L., and L. Mahrt, 1987: Interaction between soil hydrology and boundary-layer development. *Bound. Lay. Meteorol.*, **38**, 185-202, http://doi.org/10.1007/BF00121563.

- Standard reference for Noah LSM's origins

Sellers, P.J., R.E. Dickinson, D.A. Randall, A.K. Betts, F.G. Hall, J.A. Berry, G.J. Collatz, A.S. Denning, H.A. Mooney, C.A. Nobre, N. Sato, C.B. Field, and A. Henderson-Sellers, 1997: Modeling the exchanges of energy, water, and carbon between continents and the atmosphere. *Science*, **275**, 502-509, http://doi.org/10.1126/science.275.5299.502.

- Fundamental reference on land surface modeling

Chen, F. and J. Dudhia, 2001: Coupling an advanced land surface–hydrology model with the Penn State–NCAR MM5 modeling system. Part II: Preliminary model validation. *Mon. Wea. Rev.*, **129**, 587-604, http://doi.org/10.1175/1520-0493(2001)129<0587:CAALSH>2.0.CO;2.

Ek, M.B., K.E. Mitchell, Y. Lin, E. Rogers, P. Grunmann, V. Koren, G. Gayno, and J.D. Tarpley, 2003: Implementation of Noah land surface model advances in the National Centers for Environmental Prediction operational mesoscale Eta model. *J. Geophys. Res.*, **108**, 8851, http://doi.org/10.1029/2002JD003296.

- Noah LSM is used in the main operational weather forecasting model at NCEP

LeMone, M.A., M. Tewari, F. Chen, J.G. Alfieri, and D. Niyogi, 2008: Evaluation of the Noah land surface model using data from a fair-weather IHOP_2002 day with heterogeneous surface fluxes. *Mon. Wea. Rev.*, **136**, 4915-4941, http://doi.org/10.1175/2008MWR2354.1.

- Standard reference for Noah LSM performance

5.9 NARR was developed using the NCEP mesoscale Eta model and its data assimilation system, including the Noah LSM:

Chen, F., Z. Janjić, and K. Mitchell, 1997: Impact of atmospheric surface-layer parameterizations in the new land-surface scheme of the NCEP mesoscale Eta model. *Boundary-Layer Meteorol.*, **85**, 391-421, http://doi.org/10.1023/A:1000531001463.

5.10 Background on MODIS-based surface fields:

Broxton, P.D., X. Zeng, D. Sulla-Menashe, and P.A. Troch, 2014: A global land cover climatology using MODIS data. *J. Appl. Meteor. Climatol.*, **53**, 1593-1605, http://doi.org/10.1175/JAMC-D-13-0270.1.

5.11 Use of WRF with CMAQ (also good resources regarding MODIS vegetation products):

Ran, L., R. Gilliam, F. S. Binkowski, A. Xiu, J. Pleim, and L. Band, 2015: Sensitivity of the Weather Research and Forecast/Community Multiscale Air Quality modeling system to MODIS LAI, FPAR, and albedo. *J. Geophys. Res. Atmos.*, **120**, 8491-8511, http://doi.org/10.1002/2015JD023424.

Ran, L., J. Pleim, R. Gilliam, F. S. Binkowski, C. Hogrefe, and L. Band, 2016: Improved meteorology from an updated WRF/CMAQ modeling system with MODIS vegetation and albedo. *J. Geophys. Res. Atmos.*, **121**, 2393-2415, http://doi.org/10.1002/2015JD024406.

5.12 Using WRF to diagnose high-resolution, fine-scale meteorological fields:

Warner, T.T., R.A. Peterson, and R.E. Treadon, 1997: A tutorial on lateral boundary conditions as a basic and potentially serious limitation to regional numerical weather prediction. *Bull. Amer. Meteor. Soc.*, **78**, 2599-2618, http://doi.org/10.1175/1520-0477(1997)078<2599:ATOLBC>2.0.CO;2.

García-Díez, M., J. Fernández, D. San-Martín, S. Herrera, and J.M. Gutiérrez, 2015: Assessing and improving the local added value of WRF for wind downscaling. *J. Appl. Meteor. Climatol.*, **54**, 1556-1568, http://doi.org/10.1175/JAMC-D-14-0150.1.

Hon, K.-K., 2019: Predicting low-level wind shear using 200-m-resolution NWP at the Hong Kong International Airport. *J. Appl. Meteor. Climatol.*, **59**, 193–206, http://doi.org/10.1175/JAMC-D-19-0186.1.

5.13 Benefits of frequent re-initialization:

Lo, J. C.-F., Z.-L. Yang, and R.A. Pielke, 2008: Assessment of three dynamical climate downscaling methods using the Weather Research and Forecasting (WRF) model. *J. Geophys. Res. Atmos.*, **113**, http://doi.org/10.1029/2007JD009216.

Lucas-Picher, P., F. Boberg, J.H. Christensen, and P. Berg, 2013: Dynamical downscaling with reinitializations: A method to generate fine-scale climate datasets suitable for impact studies. *J. Hydrometeor.*, **14**, 1159–1174, http://doi.org/10.1175/JHM-D-12-063.1.

5.14 Various other uses of WRF:

Case, J.L., W.L. Crosson, S.V. Kumar, W.M. Lapenta, and C.D. Peters-Lidard, 2008: Impacts of high-resolution land surface initialization on regional sensible weather forecasts from the WRF model. *J. Hydrometeor.*, **9**, 1249-1266, http://doi.org/10.1175/2008JHM990.1.

Jiménez, P.A., J.F. González-Rouco, E. García-Bustamante, J. Navarro, J.P. Montávez, J.V. de Arellano, J. Dudhia, and A. Muñoz-Roldan, 2010: Surface wind regionalization over complex terrain: Evaluation and analysis of a high-resolution WRF simulation. *J. Appl. Meteor. Climatol.*, **49**, 268-287, http://doi.org/10.1175/2009JAMC2175.1.

Case, J.L., S.V. Kumar, J. Srikishen, and G.J. Jedlovec, 2011: Improving numerical weather predictions of summertime precipitation over the southeastern United States through a high-resolution initialization of the surface state. *Wea. Forecasting*, **26**, 785-807, http://doi.org/10.1175/2011WAF2222455.1.

Benjamin, S.G., S.S. Weygandt, J.M. Brown, M. Hu, C.R. Alexander, T.G. Smirnova, J.B. Olson, E.P. James, D.C. Dowell, G.A. Grell, H. Lin, S.E. Peckham, T.L. Smith, W.R. Moninger, J.S. Kenyon, and G.S. Manikin, 2016: A North American hourly assimilation and model forecast cycle: The Rapid Refresh. *Mon. Wea. Rev.*, **144**, 1669-1694, http://doi.org/10.1175/MWR-D-15-0242.1.

Fernández-González, S., M.L. Martín, E. García-Ortega, A. Merino, J. Lorenzana, J.L. Sánchez, F. Valero, and J.S. Rodrigo, 2018: Sensitivity analysis of the WRF model: Wind-resource assessment for complex terrain. *J. Appl. Meteor. Climatol.*, **57**, 733-753, http://doi.org/10.1175/JAMC-D-17-0121.1.